THE JOURNAL OF PHYSICAL CHEMISTRY B

ARTICLE

pubs.acs.org/JPCB

Quantifying the Presence of Unwanted Fluorescent Species in the Study of Pyrene-Labeled Macromolecules

Shaohua Chen,[†] Jean Duhamel,[*,†] Greg J. Bahun,[‡] and Alex Adronov[‡]

[†]Institute for Polymer Research, Department of Chemistry, University of Waterloo, Waterloo, ON N2L 3G1, Canada

[‡]Department of Chemistry and the Brockhouse Institute for Materials Research, McMaster University, Hamilton, Canada

Supporting Information

ABSTRACT: In order to mimic the effect that unwanted fluorescent species have on the process of excimer formation between pyrene labels covalently attached onto macromolecules, the steady-state fluorescence spectra and time-resolved fluorescence decays were acquired for mixtures of pyrene monolabeled and doubly end-labeled 2K poly(ethylene oxide) referred to as Py_1-PEO(2K) and Py_2-PEO(2K), respectively, and mixtures of 1-pyrenebutyric acid (PyBA) and a fourth generation dendron end-capped with pyrene (Py_{16}-G4-PS). Monolabeled polymers like Py_1-PEO(2K) and unattached fluorescent labels like PyBA are among the most typical fluorescent impurities that are encountered in the study of fluorescently labeled macromolecules. Our fluorescence experiments revealed that addition of minute amounts of Py_1-PEO(2K) or PyBA to, respectively, Py_2-PEO(2K) or Py_{16}-G4-PS solutions induced a dramatic reduction of the ratio of the fluorescence intensity of the pyrene excimer to that of the pyrene monomer, namely the I_E/I_M ratio. Although the extreme sensitivity of fluorescence in general and the I_E/I_M ratio in particular to the presence of fluorescent impurities is a great concern, it is nevertheless reassuring that this effect can be quantitatively accounted for by analyzing the fluorescence decays of the pyrene monomer and excimer globally, according to a protocol which is described in detail in this study. The experiments presented herein demonstrate the importance of studying fluorescently labeled macromolecules that are of the highest purity when probing the rapid internal dynamics of a macromolecule by fluorescence.

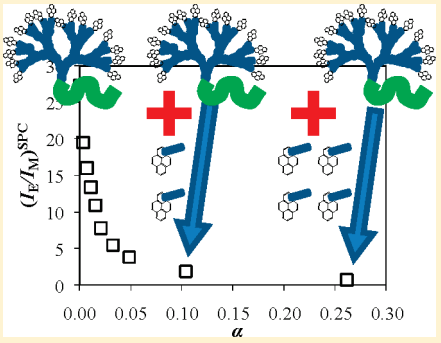

INTRODUCTION

Fluorescence dynamic quenching (FDQ) is a well-known phenomenon which has been applied in a variety of ways to estimate the rate constants for rapid processes taking place in biological or synthetic macromolecules and their supramolecular assemblies.[1] FDQ works by exciting a fluorophore which then undergoes diffusional motion, collides with a quencher and loses its excess energy (Scheme 1). In its simplest form, the rate at which the excited fluorophore loses its energy can be described by a single rate constant k_q which is typically determined by analyzing the fluorescence decay of the quenched fluorophore with a single decay time $\tau = (\tau_o^{-1} + k_q)^{-1}$, where τ_o is the natural lifetime of the fluorophore. More complicated situations involve a number n of different populations of fluorophores P_i ($0 < i < n - 1$) which are being quenched dynamically with n different rate constants k_{q_i}. Each population of fluorophore P_i decays with a single exponential whose decay time τ_i equals $(\tau_o^{-1} + k_{q_i})^{-1}$. The fluorescence decay becomes a sum of exponentials whose pre-exponential factors reflect the molar fractions f_{P_i} of the fluorophore species P_i and whose decay times τ_i yield the rate constants k_{q_i}. In turn, the rate constant k_{q_i} provides information on the environment of the fluorophore population P_i, whether P_i is accessible to or protected from the solvent, is located in a rigid or fluid environment, whereas f_{P_i} describes the molar fractions of fluorophores P_i which are in the environment defined by k_{q_i}.

Scheme 1. Quenching Mechanism between an Excited Fluorophore F* and Its Quencher Q Covalently Attached onto a Macromolecule

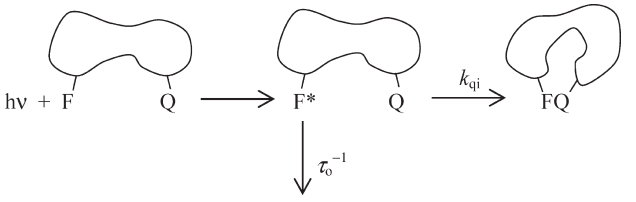

The combination of parameters f_{P_i} and k_{q_i} provides a complete description of the distribution of fluorophores and the properties of their local environment, information that is used to understand the complex behavior of macromolecules and their assemblies.[1] Important applications of these aspects of FDQ experiments include the determination of the aggregation number of surfactant micelles and a measure of their internal dynamics,[2−4] the quantitative description of long-range polymer chain dynamics,[5] or finding the fraction f_a of

Received: April 4, 2011
Revised: July 7, 2011
Published: July 29, 2011

ACS Publications © 2011 American Chemical Society

Scheme 2. Excimer Formation between Pyrenyl Groups Covalently Attached onto a Macromolecule

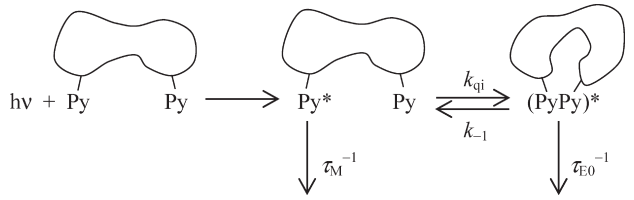

fluorophores accessible to a quencher in a protective quenching experiment.[6,7]

While FDQ experiments have proved extremely successful in the characterization of fluorescently labeled biological and synthetic macromolecules, they are limited in practice by the ability of the software used to analyze the fluorescence decays to retrieve the decay times τ_i and the fractions f_{P_i} of the fluorophore population. However, recent studies suggest that the analysis of fluorescence decays to retrieve information on complex FDQ processes is dramatically enhanced if the product of an F*−Q encounter emits with its own fluorescence as is the case with pyrene excimer formation (Scheme 2).[8−11] Upon irradiation with UV light, an excited pyrene monomer can either fluoresce with a lifetime τ_M or form an excimer with one or several rate constants which are equivalent to k_{q_i} in Scheme 1. The excimer can fluoresce with a lifetime τ_{E0} or dissociate with a rate constant k_{-1} which, for temperatures smaller than 35 °C, can be considered to be negligible.[8−11] In turn, information on the (f_{P_i}, k_{q_i}) parameters is incorporated not only in the pyrene monomer fluorescence decay but also in the pyrene excimer fluorescence decay and the pairs of (f_{P_i}, k_{q_i}) parameters are retrieved from the analysis of the pyrene monomer and excimer fluorescence decays. Experiments based on Scheme 2 have been instrumental in the study of the internal dynamics of pyrene end-labeled monodisperse polymers,[12−28] dendrimers,[29−39] and telomers with specific chain lengths.[40−42]

Some of us have applied global analysis of coupled fluorescence decays introduced some 20 years ago[43−45] to develop families of programs where both decay times and pre-exponential factors are optimized as a function of the parameters f_{P_i}, k_{q_i}, and τ_{E0} according to the fluorescence blob model,[46−56] the Birks scheme,[56,57] or the model free analysis.[47,58,59] To this date, this type of analysis has been applied successfully to determine the level of association of pyrene-labeled hydrophobically modified water-soluble polymers,[46−50] the molar absorbance coefficient of pyrene aggregates in water,[50] and the critical micelle concentration of pyrene-labeled Gemini surfactants,[59] and study the internal dynamics of linear and branched macromolecules,[52−58] the phase separation of pyrene-labeled lipids[51] and the breakdown of Birks' scheme analysis used to describe the end-to-end cyclization of a series of pyrene end-capped monodisperse poly(ethylene oxide)s.[57]

Besides the ability of this type of analysis to provide a solid description of the process of pyrene excimer formation under a wide variety of experimental conditions,[46−59] some reports also suggest that it retrieves with incredibly good accuracy the fraction $f_{free} = f_{P_0}$ of pyrene monomers that are unable to encounter a ground-state pyrene to form an excimer and for which $k_{q_0} = 0\ s^{-1}$.[57−59] These pyrenes that do not form excimer behave as if they were free in solution. For this reason, they are referred to as Py_{free} in this study and they emit with the natural lifetime of the pyrene monomer τ_M. Unfortunately, the Py_{free} species covalently attached onto a macromolecule is usually indistinguishable from the pyrene derivative used in the labeling reaction which might not have been properly removed from the fluorescently labeled macromolecule. These pyrene species act as fluorescent impurities that corrupt the fluorescence response of the labeled macromolecule. Consequently, the ability to determine f_{free} reliably for pyrene-labeled macromolecules would be an invaluable analytical tool for the quantitative description of the process of pyrene excimer formation. Furthermore, it would enable the experimentalist to gauge the extent by which the presence of Py_{free} might affect the analysis of the fluorescence data.

In order to assess the extent to which this type of analysis can determine f_{free} reliably, solutions of pyrene-labeled macromolecules were tainted with known amounts of a pyrene monomer species. Their fluorescence decays were analyzed globally and the fraction f_{free} retrieved from the analysis was compared to that expected from the amount of a pyrene monomer species purposedly added to the solution. The two pyrene-labeled macromolecules considered for this study were a 2K poly(ethylene oxide) (Py_2-PEO(2K)) and a fourth generation dendrimer hybrid (Py_{16}-G4-PS) whose ends were capped with pyrene. The solutions of Py_2-PEO(2K) and Py_{16}-G4-PS were tainted by adding a sample of PEO(2K) labeled at one end with pyrene (Py_1-PEO(2K)) and 1-pyrenebutyric acid (PyBA), respectively. Monolabeled chains such as Py_1-PEO(2K) or unattached labels such as PyBA are fluorescent impurities that are typically encountered in these types of experiments. This study describes how the global analysis of the pyrene monomer and excimer fluorescence decays handles the presence of pyrene monomer species in samples of pyrene-labeled macromolecules.

EXPERIMENTAL SECTION

Materials. The syntheses of the pyrene-labeled dendrimer hybrid (Py_{16}-G4-PS) and PEO(2K) (Py_2-PEO(2K) and Py_1-PEO)2K)), whose structures are shown in Figure 1, have been described in two earlier publications.[57,60] The Py_2-PEO(2K) and Py_{16}-G4-PS are free of unattached pyrene derivatives as determined by gel permeation chromatography in Figures S.5 and S.6 in the Supporting Information. Solutions of pyrene-labeled dendrimer and poly(ethylene oxide) were prepared with, respectively, distilled in glass tetrahydrofuran (THF) or acetone which were purchased from Caledon and used as received. 1-Pyrenebutyric acid (PyBA, 97%) was purchased from Aldrich.

Absorbance Measurements. Absorption spectra were acquired on a Cary 100 UV−vis spectrophotometer with a UV cell having a 1 cm path length. All Py_2-PEO(2K)/Py_1-PEO(2K) mixtures used in the fluorescence experiments had an absorbance smaller than 0.3, equivalent to a pyrene concentration smaller than 7×10^{-6} mol·L^{-1}. These concentrations were low enough to ensure that excimer formation occurred only intramolecularly as diluting the solution concentration by half resulted in a fluorescence spectrum that overlapped perfectly that of the more concentrated solution. All Py_{16}-G4-PS/PyBA solutions had an absorbance of 0.1.

Steady-State Fluorescence Measurements. All steady-state fluorescence spectra were acquired on a Photon Technology International (PTI) fluorometer equipped with a PTI 814 photomultiplier detection system and an Ushio UXL-75Xe xenon arc lamp as the light source. The sample solutions were degassed under a gentle flow of nitrogen for at least 30 min and all

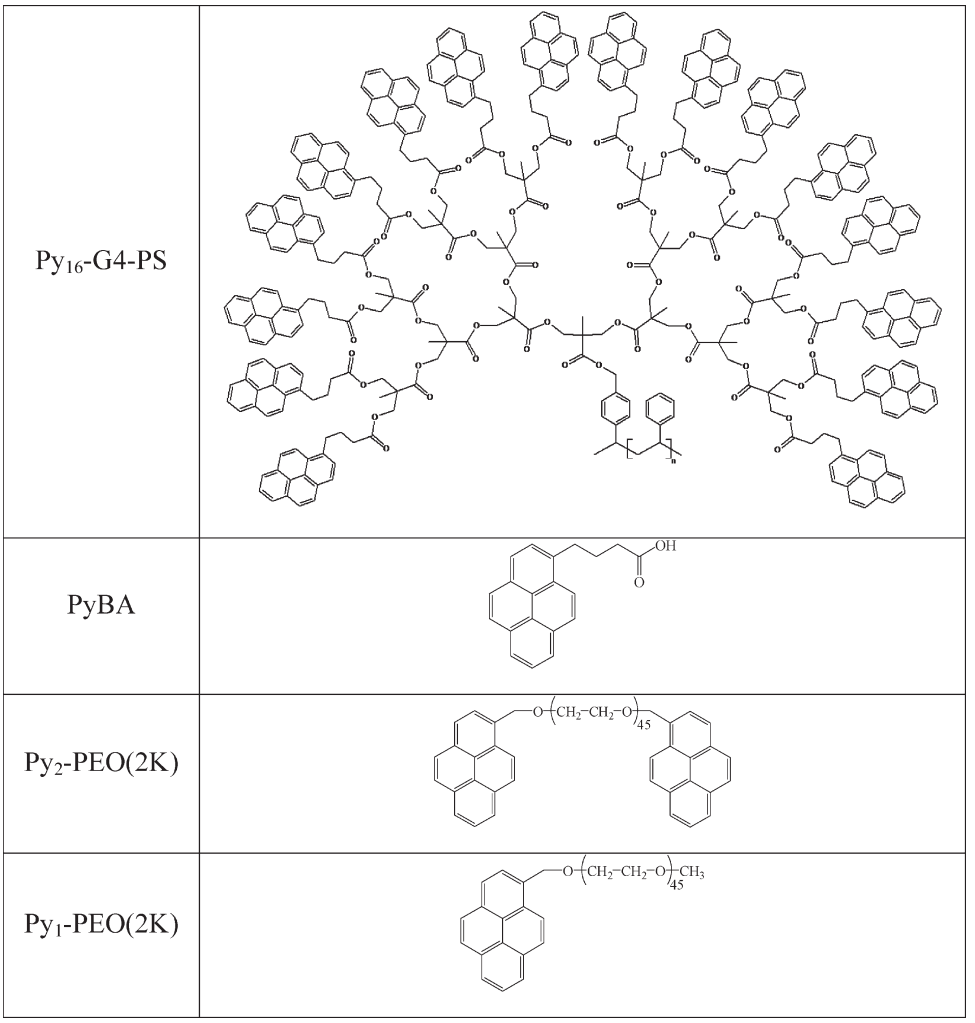

Figure 1. Chemical structures of the pyrene-labeled dendrimer hybrid (Py_{16}-G4-PS), the monolabeled (Py_1-PEO(2K)) and doubly (Py_2-PEO(2K)) labeled 2K poly(ethylene oxide)s, as well as of 1-pyrenebutyric acid (PyBA).

spectra were obtained using a quartz cuvette with the right-angle configuration. The samples were excited at a wavelength of 344 nm and all emission spectra were normalized at 375 nm. The fluorescence intensities of the monomer (I_M) and of the excimer (I_E) were estimated by taking the integrals under the fluorescence spectra from 372 to 378 nm for the pyrene monomer, and from 500 to 530 nm for the pyrene excimer, respectively. A superscript "SS" was used for the ratio of I_E over I_M $(I_E/I_M)^{SS}$ to indicate that the fluorescence intensities were obtained by steady-state fluorescence.

Time-Resolved Fluorescence Measurements. The fluorescence decay curves of the degassed samples were obtained by the time-correlated single-photon-counting technique (TC-SPC) on an IBH time-resolved fluorometer using the right-angle geometry. The excitation source was an IBH 340 nm LED used with a 500 kHz repetition rate. Fluorescence decays were acquired over 1024 channels ensuring a minimum of 20 000 counts at their maximum. The excitation wavelength was 344 nm, and the fluorescence from the pyrene monomer and excimer was monitored at 375 and 510 nm, respectively. To block potential light scattering leaking through the detection system, filters were used with cutoff wavelengths of 370 and 495 nm to obtain the fluorescence decays of the pyrene monomer and excimer, respectively. A time per channel of 2.04 ns/channel and 0.118 ns/channel was used for the Py_2-PEO(2K)/Py_1-PEO(2K) and the Py_{16}-G4-PS/PyBA mixtures, respectively. The shorter time per channel was employed to capture the short decay times observed with the dendrimer solutions.[58] For all the decays obtained by the Py_2-PEO(2K)/Py_1-PEO(2K) mixtures, reference decays of degassed solutions of PPO [2,5-diphenyloxazole] in cyclohexane (τ = 1.42 ns) for the pyrene monomer and BBOT [2,5-bis(5-*tert*-butyl-2-benzoxazolyl)thiophene] in ethanol (τ = 1.47 ns) for the pyrene excimer were used to obtain the instrument response function (IRF) via the MIMIC method[61] needed for the analyses of the monomer and excimer decays, respectively. In the case of the dendrimer solution, a Ludox solution was employed to acquire the IRF.

Analysis of the Fluorescence Decays. The monomer and excimer decays of the Py_2-PEO(2K)/Py_1-PEO(2K) mixtures in acetone were analyzed globally with Birks' Scheme (eqs S1 and S2 in the Supporting Information) and MF analysis (eqs S5 and S6). A complete derivation of the equations used to fit the fluorescence decays and the physical quantities used in this study has been provided in the Supporting Information. The lifetime τ_M in eqs S1, S2, S5, and S6 was set to equal 265 ns in the analysis of the decays as it matches the natural lifetime of Py_1-PEO(2K)

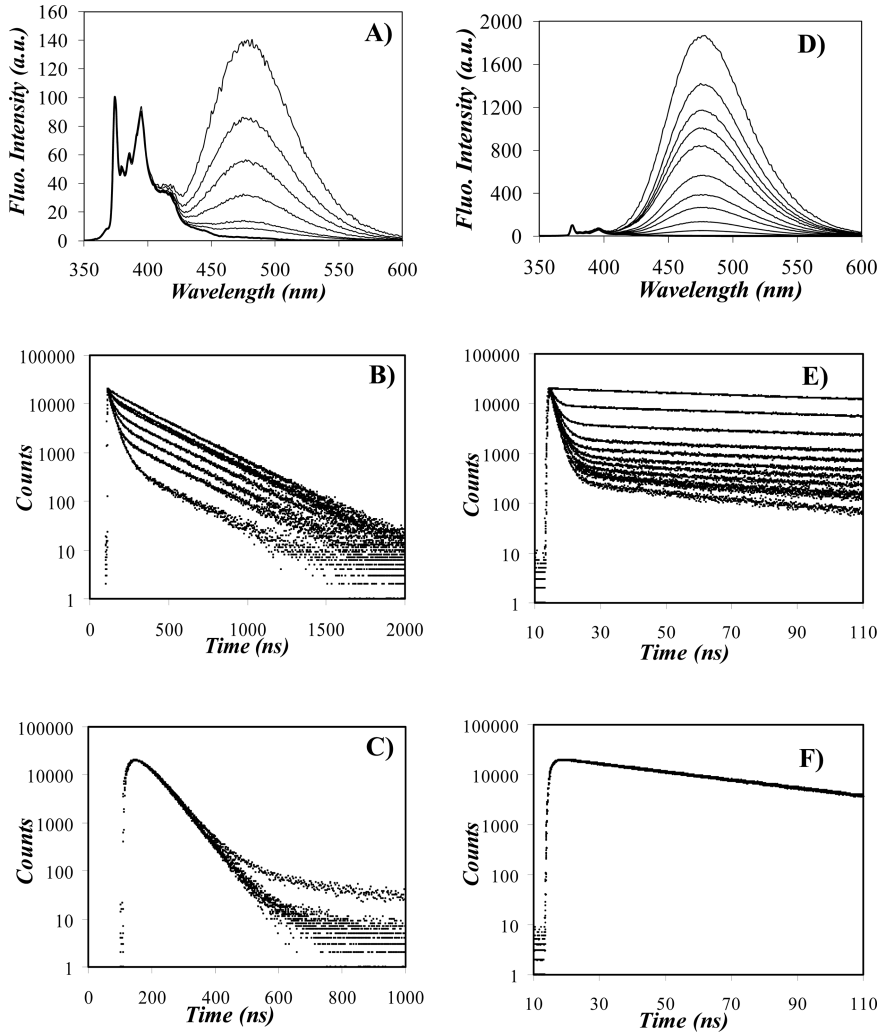

Figure 2. Left panels: Fluorescence spectra and decays of Py_2-PEO(2k)/Py_1-PEO(2k) mixtures in acetone. (A) Fluorescence spectra normalized at 375 nm; from top to bottom, $\alpha = 0$, 0.15, 0.25, 0.50, 0.70, 0.80, and 1.00. (B) Monomer fluorescence decays; $\lambda_{em} = 375$ nm; from bottom to top, $\alpha = 0$, 0.15, 0.25, 0.50, 0.70, 0.80, and 1.00. (C) Excimer fluorescence decays with that acquired for $\alpha = 0.80$ showing a substantial amount of background noise; $\lambda_{em} = 510$ nm. Right panels: Fluorescence spectra and decays of Py_{16}-G4-PS/PyBA mixtures in THF. (D) Fluorescence spectra normalized at 375 nm; from top to bottom, $\alpha = 0$, 0.05, 0.10, 0.15, 0.20, 0.25, 0.35, 0.45, 0.60, 0.70, and 1.00. (E) Monomer fluorescence decays; $\lambda_{em} = 375$ nm; from bottom to top, $\alpha = 0$, 0.05, 0.10, 0.15, 0.20, 0.25, 0.35, 0.45, 0.60, 0.70, and 1.00. (F) Excimer fluorescence decays; $\lambda_{em} = 510$ nm, $T = 23$ °C.

in acetone.[57] No short lifetime τ_{ES} was needed to fit the decays of the PEO samples. The monomer and excimer decays of the Py_{16}-G4-PS/PyBA mixtures in THF were analyzed globally with eqs S5 and S6, respectively, as Birks' scheme does not apply to the complex kinetics of excimer formation exhibited by Py_{16}-G4-PS.[58] The lifetime τ_M in eqs S5 and S6 and τ_{ES} in eq S6 were set to equal, respectively, 210 and 4 ns in the analysis. The lifetime τ_M of 210 ns for the pyrene monomer was found from the analysis of the monoexponential fluorescence decay of PyBA in THF. The lifetime τ_{ES} was estimated by letting it float in a first analysis of the fluorescence decays. It was found to fluctuate around a value of 4 ns. It was then fixed to this value in the final analysis reported in this study. The lifetime of 4 ns matches the lifetime value found for other short-lived pyrene dimers.[24,51,57,62] The analysis was carried out with the Marquardt−Levenberg algorithm[63] to obtain the optimized pre-exponential factors and decay times. The fits were good with χ^2 being smaller than 1.30, and residuals and autocorrelation of the residuals randomly distributed around zero.

RESULTS

The fluorescence spectra and decays of the Py_2-PEO(2K)/Py_1-PEO(2K) mixtures were acquired for different molar fractions α of the Py_1-PEO(2K) solution prepared with a pyrene concentration of 3.0×10^{-6} mol·L^{-1}, half that of the Py_2-PEO(2K) solution for which the pyrene concentration equals 6.0×10^{-6} mol·L^{-1}. Both concentrations are low enough to prevent intermolecular excimer formation. In effect, α which is equal to [Py_1-PEO(2K)]/([Py_1-PEO(2K)] + [Py_2-PEO(2K)]) represents the molar fraction of Py_1-PEO(2K) molecules in the Py_2-PEO(2K)/Py_1-PEO(2K) mixture. In other words, α represents the molar fraction of impurity in the mixture assuming that all macromolecules are fully labeled. The spectra are shown in Figure 2A. Based on the definition of α, a Py_2-PEO(2K)/Py_1-PEO(2K) mixture with an α value of 0.15 would have been prepared by mixing a volume fraction $100 \times [1 + (\alpha/(1 - \alpha)) \times (6.0 \times 10^{-6}$ mol·$L^{-1}/3.0 \times 10^{-6}$ mol·$L^{-1})]^{-1} = 74$ vol % of the Py_2-PEO(2K) solution with 26 vol % of the Py_1-PEO(2K)

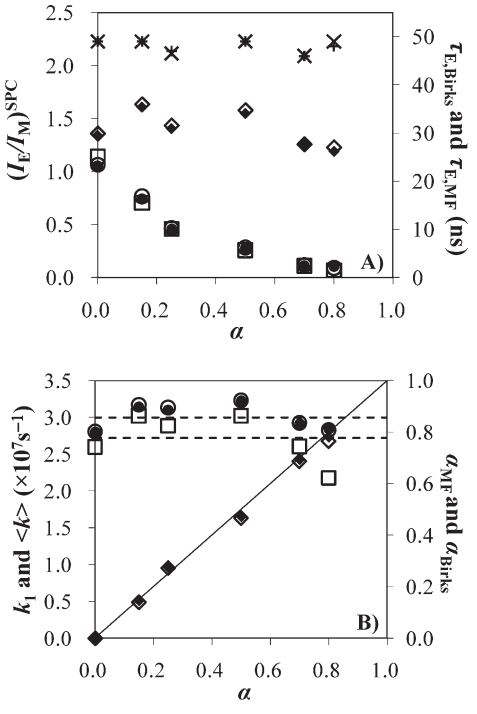

Figure 3. (A) Plot of $(I_E/I_M)^{SS}$ (□), $(I_E/I_M)^{SPC}_{Birks}$ (●), $(I_E/I_M)^{SPC}_{MF}$ (○), $(I_E/I_M)^{SPC}_{Birks,f_{free}=0}$ (◆), $(I_E/I_M)^{SPC}_{MF,f_{free}=0}$ (◇), $\tau_{E,Birks}$ (+), and $\tau_{E,MF}$ (×) as a function of the molar fraction α. (B) Plot of k_1 (●), ⟨k⟩ calculated with eq S20 (□), ⟨k⟩ calculated with eq S21 (○), α_{MF} (◇), and α_{Birks} (◆) as a function of α. T = 23 °C.

solution. Well-defined peaks were observed in the wavelength range 370−400 nm characteristic of the pyrene monomer whereas the usual excimer emission was found as a broad, structureless emission centered around 480 nm. As more Py_1-PEO(2K) is added to the Py_2-PEO(2K) solution, the excimer emission at 480 nm decreases in Figure 2A and the contribution of the 265 ns decay time characteristic of Py_1-PEO(2K) increases in Figure 2B. Residual contribution of the 265 ns decay time is clearly visible in the fluorescence decay of pure Py_2-PEO(2K), indicating the presence of trace amounts of monolabeled polymer in that sample.

All excimer fluorescence decays overlapped regardless of Py_1-PEO(2K) content in Figure 2C as expected since the pyrene excimer is generated solely by Py_2-PEO(2K). The mixtures prepared with 80% of monolabeled polymer solution emitted little at 510 nm where the excimer decays were acquired and the excimer fluorescence decay exhibited more background noise (Figure 2C).

Similar trends were observed in Figure 2D where the fluorescence spectra of the Py_{16}-G4-PS/PyBA mixtures were obtained for different molar fractions α of the PyBA solution. The Py_{16}-G4-PS and PyBA solutions had a concentration of 2.5×10^{-6} mol·L^{-1}. The high local pyrene concentration found in the dendritic hybrid resulted in efficient excimer formation with a strong excimer emission at 480 nm relative to the weak fluorescence of the pyrene monomer in the 370−400 nm range. As more PyBA was added, the contribution of the long monoexponential decay of PyBA increased in Figure 2E. However, since the excimer is formed intramolecularly by the pyrene-labeled dendrons, the excimer fluorescence decays overlapped perfectly in Figure 2F, regardless of the quantity of PyBA added to the Py_{16}-G4-PS solution.

The fluorescence spectra shown in Figure 2A were used to calculate the $(I_E/I_M)^{SS}$ ratios of the Py_2-PEO(2K)/Py_1-PEO(2K) mixtures which are plotted as a function of α in Figure 3A (hollow squares). Similar trends were obtained for the Py_2-PEO(2K)/Py_1-PEO(2K) mixtures in toluene and THF. Those results can be seen in Figures S.3 and S.4 in the Supporting Information. As expected from Figure 2A, $(I_E/I_M)^{SS}$ decreases continuously with increasing α values. The $(I_E/I_M)^{SS}$ values are relative since they depend on the specific fluorometer used, its settings, and the procedure applied to determine the fluorescence intensities $(I_M)^{SS}$ and $(I_E)^{SS}$. The $(I_E/I_M)^{SS}$ values in Figure 3A were normalized to compare them with the $(I_E/I_M)^{SPC}$ ratios determined from the parameters derived from the fluorescence decay analysis and by applying eqs S18 and S19 in the Supporting Information.

As typically done with pyrene end-labeled monodisperse polymers,[12−28] Birks' scheme was used to fit globally the monomer and excimer fluorescence decays shown in Figure 2B and C, using eqs S1 and S2.[56,57] All fits were excellent with residuals and autocorrelation of the residuals randomly distributed around zero, resulting in all χ^2 being smaller than 1.20. The parameters retrieved from the analysis have been listed in Table S.1 in the Supporting Information. In all polymer mixtures, the excimer lifetime was found to equal 48 ± 2 ns, in good agreement with the τ_{E0} value expected for pyrene excimer in organic solvents.[8,56,57] Regardless of mixture composition, the rate constant of excimer formation k_1 remained constant with α (Figure 3B), taking an average value of 3.0 (±0.2) × 10^7 s^{-1}. The constancy of k_1 with α is expected since the intramolecular excimer formation of Py_2-PEO(2K) is independent of the presence of Py_1-PEO(2K) in the mixtures. In the absence of Py_1-PEO(2K) (i.e., for α = 0), the analysis yields a molar fraction of pyrenes that do not form excimer, namely the f_{Mfree} value, of 0.034 which reflects a residual amount of monolabeled Py_1-PEO(2K) impurity in the Py_2-PEO(2K) sample. Not surprisingly, f_{Mfree} increases when increasing amounts of monolabeled sample are added to the solution (see Table S.1A).

The $(I_E/I_M)^{SPC}_{Birks}$ ratio corresponding to the I_E/I_M ratio obtained by using the parameters retrieved by analyzing the monomer and excimer fluorescence decays with Birks' scheme was calculated according to eq S18 in the Supporting Information and is plotted as a function of α (Figure 3A). As more monolabeled polymer is added to the solution, $(I_E/I_M)^{SPC}_{Birks}$ decreases. The $(I_E/I_M)^{SPC}_{Birks}$ values overlapped perfectly those obtained for $(I_E/I_M)^{SS}$ indicating that $(I_E/I_M)^{SPC}_{Birks}$ and $(I_E/I_M)^{SS}$ are in effect equivalent, the only difference being that $(I_E/I_M)^{SPC}_{Birks}$ is an absolute value whereas $(I_E/I_M)^{SS}$ is not. The $(I_E/I_M)^{SPC}_{Birks,f_{free}=0}$ ratio expected if no monolabeled polymer is present in the solution was calculated by setting in eq S18 the molar fraction of pyrenes forming excimer by diffusion, namely f_{Mdiff}, and f_{Mfree} equal to one and zero, respectively. Within experimental error, $(I_E/I_M)^{SPC}_{Birks,f_{free}=0}$ remained constant as a function of α and equal to 1.4 ± 0.2 in Figure 3A as expected since the $(I_E/I_M)^{SPC}_{Birks,f_{free}=0}$ ratio describes the amount of excimer formed intramolecularly by Py_2-PEO(2K) and it is independent of the Py_1-PEO(2K) content. It is also worth noting that $(I_E/I_M)^{SPC}_{Birks}$ = 1.05 for α = 0 is about 40% smaller than $(I_E/I_M)^{SPC}_{Birks,f_{free}=0}$ due to the presence of f_{Mfree} = 0.034 of Py_1-PEO(2K) in the Py_2-PEO(2K) sample. This represents a rather large drop in the value of the I_E/I_M ratio for the presence of a minute amount (3.4 mol %) of fluorescent impurity (Py_1-PEO(2K)). This impurity is not expected to be free unattached pyrene label as gel permeation chromatography

(GPC) of the Py_2-PEO(2K) sample conducted with a fluorescence detector indicates that it is free of low molecular weight fluorescent impurities.

The MF analysis was then applied to fit globally the monomer and excimer fluorescence decays using, respectively, eqs S5 and S6 with $n = 2$. No ES* species could be detected and their contribution was set to zero in the analysis. The fits were excellent resulting in χ^2 smaller than 1.20 and residuals and autocorrelation of the residuals randomly distributed around zero. An example of the fit of the monomer and excimer decays for the sample with $\alpha = 0.25$ can be found in Figure S.1 in the Supporting Information. The parameters retrieved from the MF analysis have been listed in Table S.2 in the Supporting Information. Only residual association between ground-state pyrene monomers could be detected amounting to a molar fraction f_{E0} of 0.04 ± 0.02. The excimer lifetime was found to equal 48 ± 2 ns, which is consistent with the τ_{E0} value obtained by the Birks' scheme analysis (Figure 3A). Moreover, the molar fractions of Py_1-PEO(2K) in solution, f_{Mfree}, listed in Tables S.1A and S.2A are identical whether they are obtained directly from Birks' scheme or MF analysis, indicating that both analyses are self-consistent.

The parameters obtained by fitting the monomer and excimer fluorescence decays with the MF analysis and listed in Table S.2 were used to calculate the $(I_E/I_M)^{SPC}_{MF}$ ratio based on eq S19. $(I_E/I_M)^{SPC}_{MF}$ is plotted as a function of α in Figure 3A. The agreement observed between the ratios $(I_E/I_M)^{SS}$, $(I_E/I_M)^{SPC}_{Birks}$, and $(I_E/I_M)^{SPC}_{MF}$ is excellent, thus confirming their equivalence. The $(I_E/I_M)^{SPC}_{MF,f_{free}=0}$ ratio expected if no monolabeled polymer is present in the solution was calculated by setting in eq S19 f_{Mdiff} and f_{Mfree} equal to 1 and 0, respectively. $(I_E/I_M)^{SPC}_{MF,f_{free}=0}$ remained constant and equal to 1.4 ± 0.2 as a function of α in Figure 3A. Within experimental error, $(I_E/I_M)^{SPC}_{Birks,f_{free}=0}$ and $(I_E/I_M)^{SPC}_{MF,f_{free}=0}$ are identical. The average rate constant $\langle k \rangle$ that provides information about the time scale over which excimer is formed by Py_2-PEO(2K) was calculated according to eqs S20 and S21. $\langle k \rangle$ was plotted as a function of α in Figure 3B and found to remain constant within experimental error and equal to 2.7 (±0.3) × 10^7 s^{-1} and 3.0 (±0.2) × 10^7 s^{-1}, respectively. The value of $\langle k \rangle$ obtained with eq S21 from the MF parameters was found to match the cyclization rate constant k_1 obtained by the Birks scheme (Figure 3A) and found to equal 3.0 (±0.2) × 10^7 s^{-1} after averaging over all the Py_2-PEO(2K)/Py_1-PEO(2K) mixtures. It suggests that eq S21 might be a better approximation to determine the average rate constant of excimer formation $\langle k \rangle$.

Most importantly, the equivalence that is expected to exist between the ratio I_E/I_M and $\langle k \rangle$ for the MF or k_1 for Birks' scheme was found to hold between $\langle k \rangle$, k_1, $(I_E/I_M)^{SPC}_{MF,f_{free}=0}$, and $(I_E/I_M)^{SPC}_{Birks,f_{free}=0}$. This equivalence was not obeyed for $(I_E/I_M)^{SS}$, $(I_E/I_M)^{SPC}_{Birks}$, and $(I_E/I_M)^{SPC}_{MF}$ since those ratios include the contribution of the monolabeled polymer. Finally, the molar fraction of the monolabeled polymer solution used to prepare the mixture (α_{Birks} or α_{MF}) could be back-calculated from the molar fraction f_{free} and f^0_{free} ($f^0_{free} = f_{free}$ when $\alpha = 0$) found with Birks' scheme or by the MF analysis of the fluorescence decays, respectively, according to eq 1.

$$\alpha_{MF} = \alpha_{Birks} = \frac{n \times (f_{free} - f^0_{free})}{n \times (f_{free} - f^0_{free}) + 1 - f_{free}} \quad (1)$$

In eq 1, n is the number of pyrene pendants attached onto the pyrene-labeled macromolecule, i.e. $n = 2$ and 16 for Py_2-PEO(2K) and Py_{16}-G4-PS, respectively. The α_{Birks} and α_{MF} values obtained by applying eq 1 were plotted as a function of α in Figure 3B for the Py_2-PEO(2K)/Py_1-PEO(2K) mixtures. The agreement observed between α_{Birks}, α_{MF}, and α is remarkable, indicating that global analysis of the monomer and excimer fluorescence decays faithfully reports on the molar fraction of Py_1-PEO(2K) that is present in the Py_2-PEO(2K)/Py_1-PEO(2K) mixtures regardless of the model used to fit the process of excimer formation. The same analysis was repeated with the fluorescence decays shown in Figure 2E,F for the Py_{16}-G4-PS/PyBA mixtures to probe further the robustness of these global analyses.

The monomer and excimer decays of the Py_{16}-G4-PS/PyBA mixtures were fitted globally with eqs S5 and S6 in the Supporting Information, respectively. Three decay times (τ_i, $i = 1-3$) were needed in both equations to handle the excimer formation by diffusion of the pyrenes attached onto the dendrimer chain ends. Two of these decay times are very small, smaller than 3 ns, suggesting that the eximer is formed by a very rapid process. To deal with the free PyBA that does not form excimer, an extra exponential was added to the expression of the monomer decay in eqs S5 with a fixed lifetime of 210 ns corresponding to that of PyBA in THF. For all solutions, an additional exponential with a decay time of 4 ns was required to fit the excimer decays. The 4 ns decay time accounts for a short-lived excimer species (ES*) which is due to either the self-quenching of some improperly stacked pyrenes or residual pyrene degradation.[24,51,57,62] All fits obtained from the global analysis of the monomer and excimer decays with the MF were good resulting in χ^2 smaller than 1.30 and residuals and autocorrelation of the residuals randomly distributed around zero (see Figure S.2 in the Supporting Information for the sample with $\alpha = 0.15$). The parameters retrieved from the analysis are listed in Table S.3. As shown in Table S.3C, the fraction of aggregated pyrenes given by f_{agg} ($= f_{E0} + f_{ES} < 0.20$) is small for all solutions, suggesting that most of the excimer is formed by the diffusive encounter between an excited and a ground-state pyrene. The excimer lifetime was found to equal 53 ± 1 ns, close to the 48 ± 2 ns lifetime found for Py_2-PEO(2K), and agrees with the τ_{E0} values found in other organic solvents.[8,56,57] The fractions of the four excited pyrene species (f_{diff}, f_{free}, f_{E_0}, and f_{ES}) were obtained using eqs S12−S15. The fraction of free PyBA (f_{free}) in Table S.3C increased with the amounts of PyBA added to the dendrimer solution, as expected.

The ratio $(I_E/I_M)^{SPC}_{MF}$ was calculated according to eq S19 and plotted as a function of the molar fraction α in Figure 4A. For the Py_{16}-G4-PS/PyBA mixtures, α equals [PyBA]/([PyBA] + [Py_{16}-G4-PS]) assuming that all pyrenes in the Py_{16}-G4-PS solutions are covalently attached onto the dendrons. The $(I_E/I_M)^{SPC}_{MF}$ trends obtained from the global analysis of the monomer and excimer fluorescence decays match perfectly the $(I_E/I_M)^{SS}$ trends calculated from the steady-state fluorescence spectra. The $(I_E/I_M)^{SPC}_{MF,f_{free}=0}$ ratio that would be expected if no free pyrene was present in the solution was calculated by setting f_{Mdiff} and f_{Mfree} equal to 1 and 0, respectively. The $(I_E/I_M)^{SPC}_{MF,f_{free}=0}$ ratio remained constant as a function of α in Figure 4A and equal to 30 ± 2, about 21 times larger than for Py_2-PEO(2K), reflecting the shorter average distance separating every two pyrenes attached onto the dendritic hybrid. The constancy of $(I_E/I_M)^{SPC}_{MF,f_{free}=0}$ is expected since it characterizes the amount of excimer formed by Py_{16}-G4-PS and it is independent of the PyBA content. $(I_E/I_M)^{SPC}_{MF,f_{free}=0}$ for $\alpha = 0$ is 20% larger than $(I_E/I_M)^{SPC}_{MF}(\alpha=0)$ due to the nonnegligible molar fraction of unattached pyrene

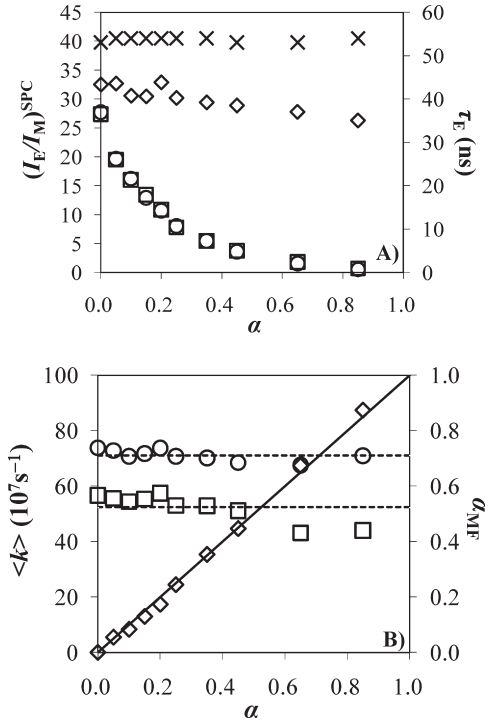

Figure 4. (A) Plot of $(I_E/I_M)^{SS}$(□), $(I_E/I_M)^{SPC}_{MF}$ (○), $(I_E/I_M)^{SPC}_{MF,f_{free}=0}$ (◇), and $\tau_{E,MF}$ (×) as a function of the molar fraction α. (B) Plot of ⟨*k*⟩ calculated with eq 20 (□), ⟨*k*⟩ calculated with eq 21 (○), and α_{MF} (◇) as a function of α. T = 23 °C.

labels (f_{free} = 0.003) present in the Py_{16}-G4-PS sample. The 20% drop in the I_E/I_M ratio due to the presence of a mere 0.3 mol % fluorescent impurity in the form of PyBA in the Py_{16}-G4-PS sample is a testimony to the outstanding sensitivity of fluorescence. It is worth pointing out that the presence of 0.3 mol % of unattached PyBA which is so easily detected in the pyrene monomer fluorescence decays shown in Figure 2E goes absolutely undetected in the GPC analysis of the Py_{16}-G4-PS sample carried out with a fluorescence detector (Figure S.6 in the Supporting Information) which fails to indicate the presence of low molecular weight fluorescent impurities.

The average rate constant ⟨*k*⟩ calculated according to eq S20 or S21 provides information about the time scale over which excimer is formed by Py_{16}-G4-PS. On the one hand, when ⟨*k*⟩ obtained with eq S20 was plotted as a function of α in Figure 4B, it remained constant within experimental error for PyBA mole fractions smaller than 50% and equal to 5.5 (±0.2) × 10^8 s^{-1} (see the lower horizontal line in Figure 4B). On the other hand, eq S21 yielded ⟨*k*⟩ values that remained constant with α and equal to 7.1 (±0.2) × 10^8 s^{-1} in Figure 4B. The improved constancy obtained for ⟨*k*⟩ by using eq S21 suggests that this equation might be more appropriate than eq S20. It must also be pointed out that eq S21 is equivalent to that used in the Birks scheme to retrieve the rate constant k_1 of excimer formation.[8] If eq S21 is applied, ⟨*k*⟩ for Py_{16}-G4-PS is 24 times larger than ⟨*k*⟩ for Py_2-PEO(2K), in agreement with the 21 fold enhancement in $(I_E/I_M)^{SPC}_{MF,f_{free}=0}$ observed between the two pyrene-labeled constructs. As was also found with the Py_2-PEO(2K) study, the similar trends that are expected between the ratio I_E/I_M and ⟨*k*⟩ are indeed observed between ⟨*k*⟩ and$(I_E/I_M)^{SPC}_{MF,f_{free}=0}$. Different trends are obtained between ⟨*k*⟩ and $(I_E/I_M)^{SS}$ or $(I_E/I_M)^{SPC}$ since those I_E/I_M ratios include the contribution of free PyBA. At high PyBA concentrations (α > 50%), ⟨*k*⟩ obtained with eq S20 and $(I_E/I_M)^{SPC}_{MF,f_{free}=0}$ deviate somewhat from their value obtained for smaller α, probably due to the significant contribution of free pyrene in this range of α values. Under these circumstances, the curvature at the start of the monomer decays which accounts for excimer formation through a rapid diffusional process is too small to be fitted accurately (Figure 2E). Furthermore, the process of pyrene excimer formation taking place in Py_{16}-G4-PS is much more complicated than that for Py_2-PEO(2K) necessitating three decay times instead of the two needed for Py_2-PEO(2K). Two out of the three decay times are also extremely small being within 3 ns. The molar fraction of the PyBA solution used to prepare the mixture (α_{MF}) could be back-calculated according to eq 22 from the fractions f_{free} and f^{o}_{free} found by the MF analysis of the fluorescence decays. It is plotted as a function of α in Figure 4B. As in Figure 3B for Py_2-PEO(2K), the agreement observed between α_{MF} and α is excellent.

To ensure that these results were not solvent-dependent, the solution of Py_2-PEO(2K)/Py_1-PEO(2K) mixtures in toluene and THF were prepared, their pyrene monomer and excimer fluorescence decays were acquired and fitted according to the MF analysis and Birks' scheme. The results of these experiments are shown in Figures S.3 and S.4 in the Supporting Information. The trends obtained are identical to those shown in Figure 3 for the Py_2-PEO(2K)/Py_1-PEO(2K) mixtures in acetone, demonstrating that the trends shown in the present study are not a function of solvent.

DISCUSSION

Although the ability of the global analyses presented in this report to retrieve quantitatively the molar fraction of a pyrene monomer species, be it PyBA or Py_1-PEO(2K), present in a sample is quite remarkable, the key advantage of these analyses resides in their ability to predict what the absolute I_E/I_M ratio should be were no pyrene monomer species present in the sample. In turn, this feature can be used to guide the experimentalist to assess the effect that the presence of a fluorescent impurity has on the fluorescence data being analyzed and whether the pyrene-labeled macromolecule needs to undergo further purification. In one particular example, this feature was fully taken advantage of to determine that the $(I_E/I_M)^{SS}$ ratio of the Py_{16}-G4 dendron was 4-fold smaller than expected because it contained a mere 3 mol % of unattached pyrene label, PyBA in this case.[58] Setting f_{free} equal to zero in eq S19 (in the Supporting Information) resulted in a $(I_E/I_M)^{SPC}_{MF,f_{free}=0}$ ratio that was 4-fold larger than $(I_E/I_M)^{SPC}_{MF}$. Another round of purification removed the unattached PyBA, and the $(I_E/I_M)^{SS}$ and $(I_E/I_M)^{SPC}_{MF}$ ratios increased 4-fold to their expected value.[58]

The dependency of the $(I_E/I_M)^{SS}$ ratio on f_{free} is illustrated in Figure 5 where $(I_E/I_M)^{SPC}$ is plotted as a function of f_{free} for different rate constants of excimer formation. The trends shown in Figure 5 were simulated by assuming that the process of excimer formation for a series of Py_2-PEO constructs of different chain lengths is well described by Birks' scheme. Using k_{-1} = 1.85 × 10^6 s^{-1}, τ_{E0} = 48 ns, τ_M = 265 ns, and the scaling relationship k_1 = 5.7 × 10^{12} × $M_n^{-1.6}$ s^{-1} which yields experimentally relevant values for Py_2-PEO in acetone,[57] eq S18 could be applied to find how the $(I_E/I_M)^{SPC}_{Birks}$ ratio varies as a function of f_{free}. The $(I_E/I_M)^{SPC}_{Birks}$ ratios normalized to their values at f_{free} = 0 show a clear trend in Figure 5. The $(I_E/I_M)^{SPC}_{Birks}$ ratio depends more

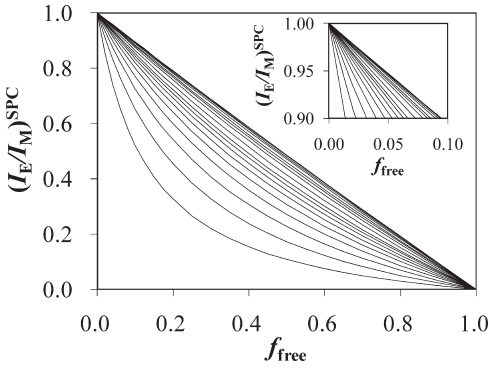

Figure 5. Simulated $(I_E/I_M)^{SPC}_{Birks}$ ratios of a series of PEOs with M_n = 2000, 3000, 4000, 5000, 6000, 7,000, 8000, 9000, 10 000, 12 000, 15 000, 17 500, 20 000, 25 000, 30 000, 35 000, 40 000 g/mol (from bottom to top) calculated with eq S18 and plotted as a function of f_{free}. Inset: zoom-in representation of the top-left corner of Figure 5.

strongly on f_{free} for larger rate constants of excimer formation. For Py_2-PEO(2K) with $k_1 = 3 \times 10^7$ s^{-1}, an f_{free} value of 0.004 (0.4 mol % unattached pyrene) is sufficient to decrease $(I_E/I_M)^{SPC}_{Birks}$ by 10%. Based on Figure 5, 3 mol % unattached pyrene or Py_1-PEO(2K) would decrease $(I_E/I_M)^{SPC}_{Birks}$ by 40% as experimentally observed in Figure 3A. On the other hand, 4 mol % of unattached pyrene (i.e., a much larger f_{free} value of 0.04) is necessary to decrease $(I_E/I_M)^{SPC}_{Birks}$ by 10% for Py_2-PEO(10K) for which $k_1 = 2.3 \times 10^6$ s^{-1}. In the case of Py_2-PEO(0.28K) with a k_1 value of 7.1×10^8 s^{-1} similar to that of Py_{16}-G4-PS, 0.06 mol % free pyrene is enough to reduce $(I_E/I_M)^{SPC}_{Birks}$ by 10%, whereas 0.3 mol % of unattached pyrene would reduce $(I_E/I_M)^{SPC}_{Birks}$ by 30%. This decrease is important as was found experimentally for Py_{16}-G4-PS for which $(I_E/I_M)^{SPC}_{MF}$ was found to be 20% smaller than expected due to the presence of 0.3 mol % of unattached 1-pyrenebutiric acid. The discrepancy between the two values (30% for the simulation versus 20% for the experiments) is due to the different kinetic schemes that are applied to compare the data shown in Figure 5 and simulated with Birks' scheme and the fluorescence decays of Py_{16}-G4-PS which were analyzed with the MF. These last examples illustrate the extreme purity that is required to obtain reliable $(I_E/I_M)^{SS}$ ratio for pyrene-labeled macromolecules that form excimer on a fast time scale, as typically found for pyrene-labeled dendrimers. It certainly rationalizes the origin of the unexpected trends often reported in studies of pyrene-labeled dendrimers, as has been suggested in a recent publication.[58]

Indeed, pyrene-labeled dendrimers have been prepared in a number of instances.[29−39] However, the majority of studies are not interested in using the excimer formation process to study the internal dynamics of the dendrimers, but rather the process of energy or electron transfer from the dendrimer periphery to its core. Consequently, little information about the $(I_E/I_M)^{SS}$ ratio or $\langle k \rangle$ is available for those pyrene-labeled dendrimers. But in the few rare instances where these parameters are reported, they often disagree. For instance, calculating the $(I_E/I_M)^{SS}$ ratio from the reported fluorescence spectra of pyrene-labeled polyester dendrimers indicates that it increases by a modest 50% when the generation number increases from 1 to 2 while the rate constant of excimer formation increases by a massive 7-fold.[38] In the case of pyrene-labeled poly(amidoamine) dendrimers, the $(I_E/I_M)^{SS}$ ratio increases by 66% when the generation number increases from 2 to 3 while $\langle \tau \rangle$ for the pyrene monomer increases from 35 to 65 ns, an implausible result which implies that $\langle k \rangle$ determined with eq S20 would decrease.[39] These observations contradict a tenant of pyrene excimer formation, namely that the rate constant of excimer formation and the I_E/I_M ratio should vary in a similar manner, as this and other studies demonstrate.[47,58,59] These inconsistencies are certainly due to the presence of pyrene fluorescent impurities that have not been taken into account in the analysis.

Since all research laboratories dealing with pyrene-labeled macromolecules use the $(I_E/I_M)^{SS}$ ratio as the main analytical tool to characterize the efficiency of a macromolecule at forming excimer,[9−11] the present study highlights in a quantitative manner the importance of ensuring and characterizing the spectral purity of a fluorescently labeled macromolecule to determine the $(I_E/I_M)^{SS}$ ratio. On the one hand, these conclusions might come as a disappointment as they illustrate the extreme sensitivity of fluorescence to the presence of minute quantities of fluorescent impurities typically found when dealing with fluorescently labeled macromolecules. On the other hand, this study represents a formidable advance forward in the investigation of fluorescently labeled macromolecules in several ways. First, the analyses presented herein take full advantage of the fact that excimer formation is being probed both in the monomer and excimer decays, so that the contribution of any emission not associated with excimer formation in the monomer decay can be determined with unmatched accuracy. As this study demonstrates, this aspect of the analysis is particularly useful to determine f_{free}. In cases where fluorophore and quencher are different and do not form a fluorescent species upon encounter as shown in Scheme 1, the analysis is weaker as it relies on the fit of the fluorophore decay only which is limited by the number of exponentials that can be used in the optimization program, usually no more than 3 for closely spaced decay times.[1] Second, the parameters obtained from the global analysis of the monomer and excimer decays can be rearranged to yield an absolute $(I_E/I_M)^{SPC}$ ratio as we have shown in eqs S18 and S19. Third, these parameters can be used to obtain the $(I_E/I_M)^{SPC}_{f_{free}=0}$ ratio which yields the value of the $(I_E/I_M)^{SPC}$ ratio free of fluorescent impurity, i.e., the parameter which is actually sought after by experimentalists. All in all, the experiments compiled in this study are expected to further enhance the use of pyrene excimer formation as being an appealing and reliable approach to study the internal dynamics of macromolecules.

■ CONCLUSIONS

The experiments presented in this study have illustrated the extreme sensitivity of fluorescence in general and the I_E/I_M ratio in particular to unwanted fluorescent impurities that are inherently present in a solution of pyrene-labeled macromolecules. The magnitudes of these effects were demonstrated with two pyrene-labeled macromolecules, namely a fourth-generation dendritic hybrid (Py_{16}-G4-PS) and a monodisperse poly(ethylene oxide) chain (Py_2-PEO(2K)) end-labeled with 16 and 2 pyrenes, respectively. In both cases, minute amounts of pyrene monomer species, 0.32 mol % of PyBA for Py_{16}-G4-PS and 3 mol % of Py_1-PEO(2K) for Py_2-PEO(2K), were found to decrease the $(I_E/I_M)^{SPC}$ ratio, and by implication the $(I_E/I_M)^{SS}$ ratio, by 20% and 40%, respectively. Although the rather large fluctuations in the I_E/I_M ratios associated with the presence of rather minute quantities of pyrene monomer species are somewhat distressful, the ability of the global analyses presented in this report at, first,

accounting quantitatively for this corrupted emission and, second, retrieving the information pertaining to excimer formation in the pyrene-labeled macromolecule, is reassuring. It is hoped that this work expands the advantages associated with the use of pyrene excimer formation to study the behavior of macromolecules in solution by fluorescence.

■ ASSOCIATED CONTENT

Supporting Information. Sample fluorescence decays of Py_2-PEO(2K)/Py_1-PEO(2K) and Py_{16}-G4-PS/PyBA mixtures; kinetic parameters retrieved from the analysis of the fluorescence decays; duplicates of Figure 3 obtained for Py_2-PEO(2K)/Py_1-PEO(2K) mixtures in toluene and THF; gel permeation chromatograms of Py_2-PEO(2K) and Py_{16}-G4-PS. This material is available free of charge via the Internet at http://pubs.acs.org.

■ ACKNOWLEDGMENT

The authors are indebted to generous funding from the National Sciences and Engineering Research Council of Canada and the Petroleum Research Fund (ACS).

■ REFERENCES

(1) Lakowicz, J. R. *Principles of Fluorescence Spectroscopy*, 3rd ed.; Springer: Singapore, 2006.
(2) Yekta, A.; Aikawa, M.; Turro, N. J. *Chem. Phys. Lett.* **1979**, *63*, 543–548.
(3) Turro, N. J.; Yekta, A. *J. Am. Chem. Soc.* **1978**, *100*, 5951–5952.
(4) Tachiya, M. *Chem. Phys. Lett.* **1975**, *33*, 289–292.
(5) Duhamel, J. *Acc. Chem. Res.* **2006**, *39*, 953–960.
(6) Hannemann, F.; Bera, A. K.; Fischer, B.; Lisurek, M.; Teuchner, K.; Bernhardt, R. *Biochemistry* **2002**, *41*, 11008–11016.
(7) Soulages, J. L.; Arrese, E. L. *Biochemistry* **2000**, *39*, 10574–10580.
(8) Birks, J. B. *Photophysics of Aromatic Molecules*; Wiley: New York, 1970; p 301.
(9) Winnik, F. M. *Chem. Rev.* **1993**, *93*, 587–614.
(10) Winnik, F. M.; Regismond, S. T. A. *Colloids Surf. A: Physicochem. Eng. Asp.* **1996**, *118*, 1–39.
(11) Duhamel, J. *Molecular Interfacial Phenomena of Polymers and Biopolymers*; Chen, P., Ed.; Woodhead: New York, 2005; pp 214— 248.
(12) Winnik, M. A. *Acc. Chem. Res.* **1985**, *18*, 73–79.
(13) Svirskaya, P.; Danhelka, J.; Redpath, A. E. C.; Winnik, M. A. *Polymer* **1983**, *24*, 319–322.
(14) Boileau, S.; Méchin, F.; Martinho, J. M. G.; Winnik, M. A. *Macromolecules* **1989**, *22*, 215–220.
(15) Ghiggino, K. P.; Snare, M. J.; Thistlethwaite, P. J. *Eur. Polym. J.* **1985**, *21*, 265–272.
(16) Cheung, S.-T.; Winnik, M. A.; Redpath, A. E. C. *Makromol. Chem.* **1982**, *183*, 1815–1824.
(17) Kim, S. D.; Torkelson, J. M. *Macromolecules* **2002**, *35*, 5943–5952.
(18) Gardinier, W. E.; Bright, F. V. *J. Phys. Chem. B* **2005**, *109*, 14824–14829.
(19) Duhamel, J.; Khayakin, Y.; Hu, Y. Z.; Winnik, M. A.; Boileau, S.; Méchin, F. *Eur. Polym. J.* **1994**, *30*, 129–134.
(20) Lee, S.; Winnik, M. A. *Macromolecules* **1997**, *30*, 2633–2641.
(21) Lee, S.; Duhamel, J. *Macromolecules* **1998**, *31*, 9193–9200.
(22) Farinha, J. P. S.; Piçarra, S.; Miesel, K.; Martinho, J. M. G. *J. Phys. Chem. B* **2001**, *105*, 10536–10545.
(23) Piçarra, S.; Gomes, P. T.; Martinho, J. M. G. *Macromolecules* **2000**, *33*, 3947–3950.
(24) Costa, T.; Seixas de Melo, J.; Burrows, H. D. *J. Phys. Chem. B* **2009**, *113*, 618–626.
(25) Cuniberti, C.; Perico, A. *Eur. Polym. J.* **1977**, *13*, 369–374.
(26) Cuniberti, C.; Perico, A. *Prog. Polym. Sci.* **1984**, *10*, 271–316.
(27) Lee, S.; Winnik, M. A. *Can. J. Chem.* **1993**, *71*, 1216–1224.
(28) Lee, S.; Winnik, M. A. *Can. J. Chem.* **1994**, *72*, 1587–1595.
(29) Ahn, T.-S.; Nantalaksakul, A.; Dasari, R. R.; Al-Kaysi, R. O.; Müller, A. M.; Thayumanavan, S.; Bardeen, C. J. *J. Phys. Chem. B* **2006**, *110*, 24331–24339.
(30) Gu, T.; Whitesell, J. K.; Fox, M. A. *J. Phys. Chem. B* **2006**, *110*, 25149–25152.
(31) Cicchi, S.; Fabbrizzi, P.; Ghini, G.; Brandi, A.; Foggi, P.; Marcelli, A.; Righini, R.; Botta, C. *Chem.—Eur. J.* **2009**, *15*, 754–764.
(32) Baker, L. A.; Crooks, R. M. *Macromolecules* **2000**, *33*, 9034–9039.
(33) Wang, B.-B.; Zhang, X.; Yang, L.; Jia, X.-R.; Ji, Y.; Li, W.-S.; Wei, Y. *Polym. Bull.* **2006**, *56*, 63–74.
(34) Modrakowski, C.; Flores, S. C.; Beinhoff, M.; Schlüter, A. D. *Synthesis* **2001**, *14*, 2143–2155.
(35) Brauge, L.; Vériot, G.; Franc, G.; Deloncle, R.; Caminade, A.-M.; Majoral, J.-P. *Tetrahedron* **2006**, *62*, 11891–11899.
(36) Brauge, L.; Caminade, A.-M.; Majoral, J.-P.; Slomkowski, S.; Wolszczak, M. *Macromolecules* **2001**, *34*, 5599–5606.
(37) Stewart, G. M.; Fox, M. A. *J. Am. Chem. Soc.* **1996**, *118*, 4354–4360.
(38) Wilken, R.; Adams, J. *Macromol. Rapid Commun.* **1997**, *18*, 659–665.
(39) Wang, B.-B.; Zhang, X.; Jia, X.-R.; Li, Z.-C.; Ji, Y.; Yang, L.; Wei, Y. *J. Am. Chem. Soc.* **2004**, *126*, 15180–15194.
(40) Zachariasse, K. A.; Duveneck, G.; Busse, R. *J. Am. Chem. Soc.* **1984**, *106*, 1045–1051.
(41) Zachariasse, K. A.; Duveneck, G. *J. Am. Chem. Soc.* **1987**, *109*, 3790–3792.
(42) Maçanita, A. L.; Zachariasse, K. A. *J. Phys. Chem. A* **2011**, *115*, 3183–3195.
(43) Andriessen, R.; Boens, N.; Ameloot, M.; De Schryver, F. C. *J. Phys. Chem.* **1991**, *95*, 2047–2058.
(44) Andriessen, R.; Ameloot, M.; Boens, N.; De Schryver, F. C. *J. Phys. Chem.* **1992**, *96*, 314–326.
(45) Boens, N.; Ameloot, M. *Int. J. Quantum Chem.* **2006**, *106*, 300–315.
(46) Siu, H.; Duhamel, J. *Macromolecules* **2004**, *37*, 9287–9289.
(47) Siu, H.; Duhamel, J. *J. Phys. Chem. B* **2005**, *109*, 1770–1780.
(48) Siu, H.; Duhamel, J. *Macromolecules* **2005**, *38*, 7184–7186.
(49) Siu, H.; Duhamel, J. *Macromolecules* **2006**, *39*, 1144–1155.
(50) Siu, H.; Duhamel, J. *J. Phys. Chem. B* **2008**, *112*, 15301–15312.
(51) Siu, H.; Duhamel, J.; Sasaki, D.; Pincus, J. L. *Langmuir* **2010**, *26*, 10985–10994.
(52) Ingratta, M.; Duhamel, J. *Macromolecules* **2007**, *40*, 6647–6657.
(53) Ingratta, M.; Duhamel, J. *J. Phys. Chem. B* **2008**, *112*, 9209–9218.
(54) Ingratta, M.; Duhamel, J. *J. Phys. Chem. B* **2009**, *113*, 2284–2292.
(55) Ingratta, M.; Mathew, M.; Duhamel, J. *Can. J. Chem.* **2010**, *88*, 217–227.
(56) Ingratta, M.; Hollinger, J.; Duhamel, J. *J. Am. Chem. Soc.* **2008**, *130*, 9420–9428.
(57) Chen, S.; Duhamel, J.; Winnik, M. A. *J. Phys. Chem. B* **2011**, *115*, 3289–3302.
(58) Yip, J.; Duhamel, J.; Bahun, G.; Adronov, A. *J. Phys. Chem. B* **2010**, *114*, 10254–10265.
(59) Keyes-Baig, C.; Duhamel, J.; Wettig, S. *Langmuir* **2011**, *27*, 3361–3371.
(60) Bahun, G. J.; Adronov, A. *J. Polym. Sci. A: Polym. Chem.* **2010**, *48*, 1016–1028.
(61) James, D. R.; Demmer, D. R.; Verall, R. E.; Steer, R. P. *Rev. Sci. Instrum.* **1983**, *54*, 1121–1130.
(62) Piçarra, S.; Gomes, P. T.; Martinho, J. M. G. *Macromolecules* **2000**, *33*, 3947–3950.
(63) Press, W. H.; Flannery, B. P.; Teukolsky, S. A.; Vetterling, W. T. *Numerical Recipes. The Art of Scientific Computing (Fortran Version)*; Cambridge University Press: Cambridge, UK, 1992.